

A Method for Predicting Longitudinal Stability Derivatives of Rigid and Elastic Airplanes

J. ROSKAM*

University of Kansas, Lawrence, Kansas

AND

A. DUSTO†

The Boeing Company, Seattle, Wash.

Using the concept of aerodynamic and structural influence coefficients, a method for estimating longitudinal stability derivatives for rigid and elastic airplanes is presented. The airplane is divided into a large number of surface panels. From elementary solutions to the classical small perturbation, steady flow equation a matrix of aerodynamic influence coefficients is generated which is used to compute pressure distribution, total forces and moments in subsonic and supersonic flow. The elastic properties of the airplane are represented by a flexibility influence coefficient matrix. Matrix algebra is used to obtain explicit expressions for longitudinal α -, u -, and q -stability derivatives. To validate this method, comparisons are shown with tunnel data for α - and u -derivatives obtained with a rigid model of the Boeing 707 and with rigid and elastic models of a variable sweep SST configuration. The agreement between theory and tunnel data is demonstrated to be quite good.

Nomenclature

\mathbf{r}	= vector locating a point on the surface relative to the origin of the X, Y, Z system
$\boldsymbol{\omega}$	= rotational velocity vector of the airplane
ϕ'	= small perturbation velocity potential
U_∞, U_1, V_c	= freestream velocity
x, y, z	= body fixed coordinate system
u, v, w	= small perturbation velocity components in xyz
A	= aerodynamic influence coefficient
F_A, f_A	= aerodynamic pressure force (total and perturbed, respectively)
\bar{q}	= dynamic pressure
θ	= pitch attitude
α	= angle of attack
$q = \dot{\theta}$	= pitch rate
m_i	= mass of element (or panel) i
S_w	= wing reference area
\bar{c}	= wing reference chord
\mathbf{d}	= elastic displacement vector
C_θ	= structural influence coefficient

Subscripts

W	= wing
B	= body
s	= stability
V	= vortex
m	= pitching moment
D	= doublet, drag
L	= lift
1	= steady state
A	= aerodynamic
C	= center of gravity
E	= elastic, elastic surface
I	= inertial
P	= perturbation
J	= jig

Matrix

$\begin{Bmatrix} \end{Bmatrix}$	= column matrix
$\begin{bmatrix} \end{bmatrix}$	= square matrix
$\begin{bmatrix} \end{bmatrix} \begin{bmatrix} \end{bmatrix}$	= diagonal matrix

1. Introduction

THE purpose of this article is to present and discuss a technique for predicting longitudinal stability derivatives for rigid and elastic airplanes. This highly successful technique is based on a recently developed aerodynamic influence coefficient method. It will be shown that the method applies to arbitrary configurations inside the flow regime within which the linearized flow equations are valid. This means for typical airplane configurations a Mach range of approximately $0 < M < 0.8$ and $1.2 < M < 5$, the size of the transonic exclusion depending on the configuration.

Earlier work in this area, by Gainer and Aiken, was reported in Ref. 1. These authors employed a lifting line theory to calculate steady-state span loading distributions on flexible wings in subsonic flight.

The current method is founded upon an application of aerodynamic influence coefficients as developed by Woodward in Ref. 2. This way it has become possible to extend the basic ideas of Ref. 1 to encompass most longitudinal stability derivatives of airplanes and do this for both subsonic and supersonic flight. A procedure to compute stability derivatives from influence coefficients was described and validated in Ref. 3, to which the current authors also contributed. The method of this article is different in that here a consistent explicit formulation of longitudinal stability derivatives is presented.

A brief introduction to some of the properties of aerodynamic influence coefficients is presented in Sec. 2. Some comments on how structural influence coefficients enter the problem are presented in Sec. 3. With these concepts of aerodynamic and structural influence coefficients, a series of matrix expressions are derived for longitudinal α -, u -, and q -stability derivatives. Derivation of these expressions is presented in Sec. 4. To show the accuracy of the method

Presented as Paper 69-131 at the AIAA 7th Aerospace Sciences Meeting, New York, January 20-22, 1969; submitted February 3, 1969; revision received June 26, 1969. Work supported in part by NASA-Ames Contract NAS 2-3662.

* Associate Professor, Aerospace Engineering. Associate Fellow AIAA.

† Research Specialist, Aerodynamics Staff. Member AIAA.

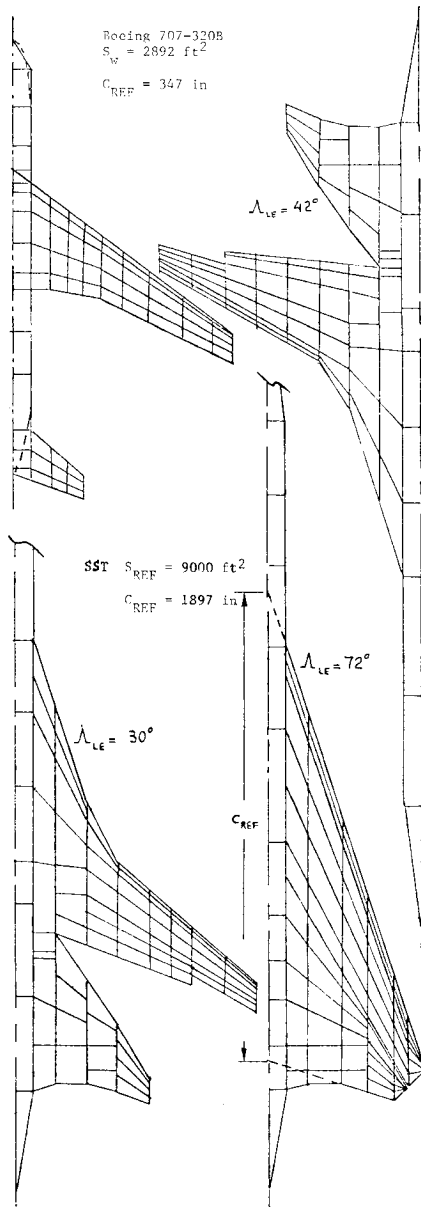


Fig. 1 Examples of panel geometries.

in predicting derivatives, a comparison with wind-tunnel data is provided in Sec. 5. Finally, in Sec. 6, conclusions are presented.

2. Aerodynamic Influence Coefficient Theory

The purpose of this section is to describe those features of the aerodynamic influence coefficient method of Ref. 2 that were utilized in the generation of stability derivatives. That aerodynamic influence coefficient method is based on elementary solutions to the small perturbation, steady flow equation:

$$\nabla^2 \phi' - M_\infty^2 (\partial^2 \phi' / \partial x^2) = 0 \quad (1)$$

where ϕ' is the small perturbation velocity potential such that

$$\begin{aligned} u' &= U_\infty (\partial \phi' / \partial x), \quad v' = U_\infty (\partial \phi' / \partial y) \\ w' &= U_\infty (\partial \phi' / \partial z) \end{aligned} \quad (2)$$

and U_∞ , M_∞ are freestream velocity and Mach number. Equation (1) represents a first-order approximation that is

valid for subsonic and supersonic flow provided

$$u'/U_\infty \ll 1, v'/U_\infty \ll 1, w'/U_\infty \ll 1 \quad (3)$$

The approximation fails in the transonic and hypersonic flow regimes. Therefore, the aerodynamic influence coefficients as well as the stability derivatives computed from them are similarly restricted.

The airplane is divided into a large number of segments as shown in Fig. 1. Segments at the wing, fuselage and tail are represented by panels of zero thickness at the chord planes. Although thickness of wing, fuselage and tail is not accounted for in this work, it is shown in Ref. 2 that this does not lead to any particular difficulty.

Flow incidence due to local camber and angle of attack is accounted for by pressures on the panels which are of constant magnitude over each panel. These are vortex sheets with uniform intensity over each panel. An important feature of the method of Ref. 2 is the inclusion of their wakes in the representation.

The aerodynamic pressure forces at the various segments due to the perturbation flow may be determined using the linearized Bernoulli equation. The pressure force at the i th segment is denoted by F_{A_i} with direction along the unit normal vector \mathbf{n}_i at the i th panel. The flow incidence due to camber and angle of attack is denoted by ψ_i . The aerodynamic pressure force at the i th panel is found as

$$F_{A_i} = \bar{q} \sum_{j=1}^n A_{ij} \psi_j \quad (4)$$

where A_{ij} represents the aerodynamic influence coefficients due to camber and angle of attack and n is the total number of panels.

The small disturbance aerodynamic pressure forces generated by small disturbance motion from a reference motion of the airplane are the aerodynamic forces associated with stability derivatives. These may be found from the aerodynamic influence coefficients by noting that the surface boundary condition for flow about a solid body is given by

$$dG/dt = 0 \text{ on } G(x_s, y_s, z_s, t) = 0 \quad (5)$$

where $G(x_s, y_s, z_s, t) = 0$ describes the surface in terms of the stability axis system. Expansion of Eq. (5) gives

$$\partial G / \partial t + \mathbf{V}_s \cdot \nabla G = 0 \text{ on } G(x_s, y_s, z_s, t) = 0 \quad (6a)$$

The time dependence is due to elastic deformation. The partial derivatives with respect to time may be removed by using the additional condition

$$\partial G / \partial t + \dot{\mathbf{d}} \cdot \nabla G = 0 \text{ on } G(x_s, y_s, z_s, t) = 0 \quad (6b)$$

The boundary condition for the elastic airplane is then found as

$$(\mathbf{V}_s - \ddot{\mathbf{d}}) \cdot \nabla G = 0 \text{ on } G(x_s, y_s, z_s, t) = 0 \quad (7)$$

Evaluating this expression at the control points and noting that $\mathbf{n} = \nabla G / (\nabla G \cdot \nabla G)^{1/2}$, it follows that

$$(\mathbf{V}_{s_i} - \dot{\mathbf{d}}_i) \cdot \mathbf{n}_i = 0 \quad (8)$$

The aerodynamic influence coefficients are obtained from elementary solutions to Eq. (1), the flow equation. For the flow equation to have the form given by Eq. (1) the coordinate system x, y, z must be an inertial frame of reference. Thus, to utilize the boundary condition as given by Eq. (8) make the x, y, z axis system nonrotating and translating at constant speed equal to that of the airplane along its x_s axis at the instant of time when stability is to be assessed, $t = t_0$.

Further, let

$$x = -x_s, \quad y = y_s, \quad \text{and } z = -z_s \text{ at } t = t_0 \quad (9)$$

Now, the velocities of a fluid particle at \mathbf{r} relative to the two systems are related as

$$\mathbf{V} = \mathbf{V}_c + U\mathbf{i} + \boldsymbol{\omega} \times \mathbf{r} + \mathbf{V}_s \quad (10)$$

But, in terms of the perturbation velocity potential,

$$\mathbf{V} = U\mathbf{i} + U\nabla\phi' \quad (11)$$

Thus, the boundary condition at the i th control point may be written as

$$(U\nabla\phi' - \mathbf{V}_c - \boldsymbol{\omega} \times \mathbf{r} - \dot{\mathbf{d}})_i \cdot \mathbf{n}_i = 0 \quad (12)$$

$$\text{for } \tilde{G}(x, y, z, t) = 0$$

where $\tilde{G}(x, y, z, t) = G[x_s(x), y_s(y), z_s(z), t] = 0$. It may be noted that the perturbation velocity potential ϕ' is required to be an explicit function of time in Eq. (12) if the velocity components are to vary with time. However, the unsteady terms have been deleted from the flow equation, Eq. (1), which forms the basis of the aerodynamic influence coefficients. One of two assumptions must therefore be introduced. Either the unsteady aerodynamic effects are assumed second order or the explicit time dependence is assumed separable and accounted for independently.

The flow incidence angle in terms of the perturbation velocity potential is found from the small angle approximation

$$\psi_i \approx \mathbf{n}_i \cdot (\nabla\phi')_i \quad (13)$$

so that Eq. (12) may be written as

$$\psi_i = (1/U)\mathbf{n}_i \cdot (\mathbf{V}_c + \boldsymbol{\omega} \times \mathbf{r} + \dot{\mathbf{d}})_i \quad (14)$$

at the control points.

The elastic deformation giving rise to change in thickness is assumed to be negligible. Thus, the flow incidence represented by Eq. (14) is, to that approximation, entirely an angle of attack and camber effect. The aerodynamic force Eq. (4) may therefore be written as

$$F_{Ai} = \bar{q} \sum_{j=1}^n A_{ij}(\mathbf{n}_j/U) \cdot (\mathbf{V}_c + \boldsymbol{\omega} \times \mathbf{r} + \dot{\mathbf{d}})_j \quad (15)$$

The small disturbance aerodynamic pressure forces are obtained by evaluating Eq. (15) for the reference and for the small disturbance motions. In doing this it must be noted that the aerodynamic influence coefficients are computed for Mach numbers which differ in the two cases. To first-order approximation this is accounted for as

$$A_{ij} \approx (A_{ij})_1 + (\partial A_{ij}/\partial M)M_1 u/U_1 \quad (16)$$

Also, the surface unit normal vectors differ as a consequence of small elastic rotations $\boldsymbol{\theta}_{Ei}$ arising from the different structural loads in the two motions. Thus, to first-order approximation

$$\mathbf{n}_i \approx \mathbf{n}_{i1} + (\boldsymbol{\theta}_E \times \mathbf{n}_i)_i \quad (17)$$

Finally, a change in dynamic pressure occurs which leads to

$$\bar{q} = \bar{q}_1 + 2\bar{q}_1 u/U_1 \quad (18)$$

Introducing these results into Eq. (15), deleting products of small quantities, and requiring satisfaction of Eq. (15) in the reference motion leads to the following result:

$$f_{Ai} = \bar{q}_1 \sum_{j=1}^n \left[2(A_{ij})_1 + M_1 \left(\frac{\partial A_{ij}}{\partial M} \right)_1 \right] \{\psi_{ij}\} \frac{u}{U_1} + \bar{q}_1 \sum_{j=1}^n [A_{ij}] \{ \mathbf{i} \cdot (\boldsymbol{\theta}_E \times \mathbf{n}_i) + \mathbf{n}_{i1} \cdot (\mathbf{v}_p + \boldsymbol{\omega}_p \times \mathbf{r}_1 + \dot{\mathbf{d}}_j) \} \quad (19)$$

The column matrix $\{\psi_{ij}\}$ represents flow incidence due to

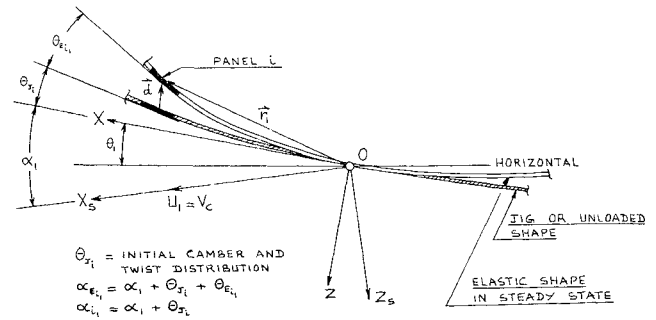


Fig. 2 Elastic airplane geometry.

camber and angle of attack in the reference motion. The panel incidence angles due to camber in the reference flight condition represent the so-called equilibrium or steady-state shape of the airplane. No restrictions have been placed on the reference or disturbed motions except that they lead to flow incidence angles that are small and that unsteady aerodynamic effects may be accounted for separately. In Sec. 4, Eq. (19) will be specialized to perturbed motion relative to steady level flight so that longitudinal stability derivatives can be derived.

3. Structural Influence Coefficient Theory

Structural deflections enter the surface boundary condition on the flow in two ways. The velocity relative to the stability axis system due to elastic displacement rate is given by the vectors $\dot{\mathbf{d}}_i$ (see Fig. 2). The change in slope of the surface due to elastic deformation is given by the small rotation vectors $\boldsymbol{\theta}_{Ei}$. The components of both of these vectors are related to structural loads by structural influence coefficients.

The precise manner in which the structure influence coefficients are derived from the theory of elastic structures is beyond the scope of this paper. This subject is further discussed in Ref. 3. It is sufficient to note that the displacement \mathbf{d}_i and rotation $\boldsymbol{\theta}_{Ei}$ are average values for the i th surface panel. The loads due to aerodynamics, inertia, and gravity which cause structural deflection are summed at each surface panel and are denoted by \mathbf{F}_i for the i th panel. Couples that may be acting at the panels due to eccentricity in the applied loads are neglected. Finally, the structural influence coefficients are defined such that

$$\{\mathbf{d}_i\} = [C_{dij}]\{\mathbf{F}_j\} \text{ and } \{\boldsymbol{\theta}_{Ei}\} = [C_{\theta ij}]\{\mathbf{F}_j\} \quad (20)$$

Only the second expression is needed in deriving quasi-steady stability derivatives for an elastic airplane. This is because the term containing $\dot{\mathbf{d}}_i$ in Eq. (20) disappears when dealing with quasi-steady stability derivatives.

4. Derivation of Longitudinal Stability Derivatives for Rigid and Elastic Airplanes

The objective of this section is to derive and discuss explicit expressions for the quasi-steady longitudinal stability derivatives of rigid and elastic airplanes. Aerodynamic influence coefficient theory and the boundary conditions as described in Sec. 2 (specialized for a reference motion of steady level flight) are used to obtain the aerodynamic load distribution over the airplane. Due to the restriction to longitudinal disturbance motion, any elastic rotations about the z and x axes are ignored as are displacements in the y and x directions. The precise geometry used in relating panel loads to panel flow incidence angles is described in Fig. 2. For reasons of economy the derivation will be presented for the elastic airplane only. By assuming a zero structural

Table 1 Longitudinal stability derivatives for rigid and elastic airplanes

Elastic	Rigid
$C_{x\alpha} = -1/S_w \{ \alpha_{E_{i1}} \}^T [B] [A] \{ 1 \}$	$= -1/S_w \{ \alpha_{i1} \}^T [A] \{ 1 \}$
$C_{xq} = 2/S_w \bar{c} \{ \alpha_{E_{i1}} \}^T [B] [A] \{ X_i \} - [C_\theta] \{ m_i \} U_1^2$	$= 2/S_w \bar{c} \{ \alpha_{i1} \}^T [A] \{ X_i \}$
$C_{xu} = -1/S_w \{ \alpha_{E_{i1}} \}^T [B] [2[A] + M_1 [\partial A / \partial M]] \{ \alpha_{E_{i1}} \}$	$= -1/S_w \{ \alpha_{i1} \}^T [2[A] + M_1 [\partial A / \partial M]] \{ \alpha_{i1} \}$
$C_{z\alpha} = -1/S_w \{ 1 \}^T [B] [A] \{ 1 \}$	$= -1/S_w \{ 1 \}^T [A] \{ 1 \}$
$C_{zq} = 2/S_w \bar{c} \{ 1 \}^T [B] [A] \{ X_i \} - [C_\theta] \{ m_i \} U_1^2$	$= 2/S_w \bar{c} \{ 1 \}^T [A] \{ X_i \}$
$C_{zu} = -1/S_w \{ 1 \}^T [B] [2[A] + M_1 [\partial A / \partial M]] \{ \alpha_{E_{i1}} \}$	$= -1/S_w \{ 1 \}^T [2[A] + M_1 [\partial A / \partial M]] \{ \alpha_{i1} \}$
$C_{m\alpha} = 1/S_w \bar{c} \{ X_i \}^T [B] [A] \{ 1 \}$	$= 1/S_w \bar{c} \{ X_i \}^T [A] \{ 1 \}$
$C_{mq} = -2/S_w \bar{c} \{ X_i \}^T [B] [A] \{ X_i \} - [C_\theta] \{ m_i \} U_1^2$	$= -2/S_w \bar{c} \{ X_i \}^T [A] \{ X_i \}$
$C_{mu} = 1/S_w \bar{c} \{ X_i \}^T [B] [2[A] + M_1 [\partial A / \partial M]] \{ \alpha_{E_{i1}} \}$	$= 1/S_w \bar{c} \{ X_i \}^T [2[A] + M_1 [\partial A / \partial M]] \{ \alpha_{i1} \}$
Elastic airplane inertial stability derivatives	
$C_{x\theta} = 1/S_w \{ \alpha_{E_{i1}} \}^T [B] [A] [C_\theta] \{ m_i \} g \sin \theta_1$	$C_{x\theta} = 1/S_w \{ 1 \}^T [B] [A] [C_\theta] \{ m_i \} g \sin \theta_1$
$C_{m\theta} = -1/S_w \bar{c} \{ X_i \}^T [B] [A] [C_\theta] \{ m_i \} g \sin \theta_1$	$C_{x\dot{q}} = -1/S_w \{ \alpha_{E_{i1}} \}^T [B] [A] [C_\theta] \{ m_i X_i \}$
$C_{x\dot{q}} = -1/S_w \{ 1 \}^T [B] [A] [C_\theta] \{ m_i X_i \}$	$C_{m\dot{q}} = 1/S_w \bar{c} \{ X_i \}^T [B] [A] [C_\theta] \{ m_i X_i \}$
$C_{x\dot{w}} = 1/S_w \{ \alpha_{E_{i1}} \}^T [B] [A] [C_\theta] \{ m_i \}$	$C_{x\dot{w}} = 1/S_w \{ 1 \}^T [B] [A] [C_\theta] \{ m_i \}$
$C_{m\dot{w}} = -1/S_w \bar{c} \{ X_i \}^T [B] [A] [C_\theta] \{ m_i \}$	

influence coefficient matrix it is possible to recover the results for a rigid airplane, as will be demonstrated.

Aerodynamic Forces

It was noted in Sec. 2 that the flow equation, Eq. (1), is written for different freestream velocities in the reference and in the disturbed states. Thus, with the aerodynamic

influence coefficient theory of Sec. 3 it is possible to write the column matrix of aerodynamic forces viewed as the sum of steady-state and perturbed forces

$$\{ F_{Ai1} + f_{Ai} \} = (\bar{q}_1 + \bar{q}) [A + (\partial A / \partial M) (M_1 / U_1) \mu] \times \{ \alpha_{E_{i1}} + \alpha_{Ei} \} \quad (21)$$

where subscript i indicates panel i , with $i = 1, 2, \dots, n$. Subscript 1 indicates a steady-state (ss) quantity. Lower case symbols alone indicate perturbed state (ps) quantities.

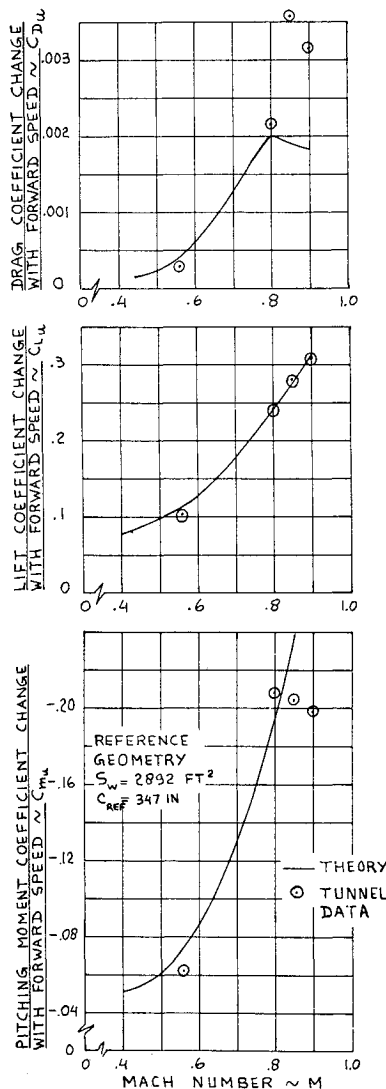


Fig. 3 Correlation of theory and tunnel data for the speed stability derivatives of the Boeing 707-320B (rigid).

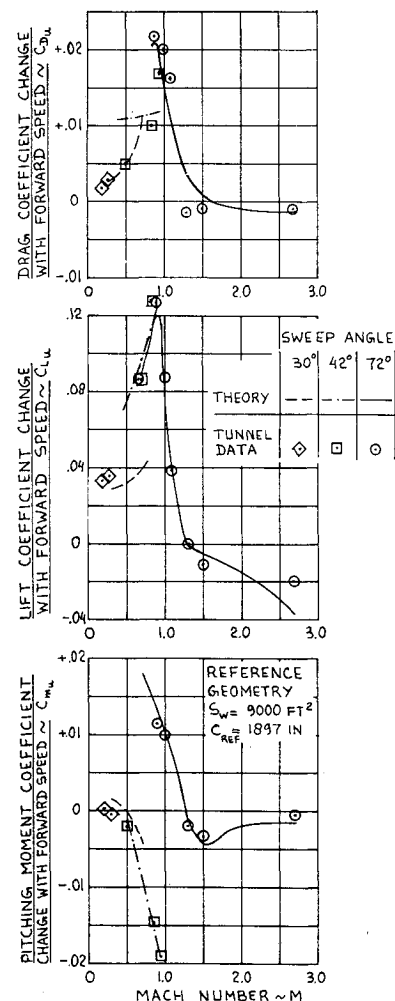


Fig. 4 Correlation of theory and tunnel data for the speed stability derivatives of an SST configuration (rigid).

It may be shown that the perturbation dynamic pressure \bar{q} can be written as

$$\bar{q} = 2\bar{q}_1 (u/U_1) \quad (22)$$

Equation (21) assumes that the only perturbation of the aerodynamic influence coefficient matrix is caused by a Mach number perturbation. Expanding Eq. (21), neglecting second-order terms, and dropping the steady-state terms results in the following expression for the column matrix of perturbed aerodynamic forces:

$$\{f_{Ai}\} = \bar{q}_1[(2/U_1)[A] + (M_1/U_1)[\partial A/\partial M]] \times \{\alpha_{Ei}\} u + q_1[A]\{\alpha_{Ei}\} \quad (23)$$

It is seen that the perturbed aerodynamic forces depend on the steady-state panel flow incidence distribution $\{\alpha_{Ei}\}$. In the following analysis, it is assumed that this matrix is known. This implies that the steady-state shape of the airplane is completely defined. A method that can be used to compute this equilibrium shape has been presented in Ref. 3. Reference 4 shows some results that indicate that the steady-state shape can indeed be accurately computed.

The matrix of perturbed panel flow incidence angles is obtained by specializing Eq. (14) to find

$$\{\alpha_{Ei}\} = \alpha\{1\} - (\dot{\theta}/U_1)\{x_i\} + \{\theta_{Ei}\} \quad (24)$$

where $\alpha = w'/U_1$ is the perturbed angle of attack of the airplane; $\dot{\theta} = q$ is the perturbed pitch rate of the airplane; θ_{Ei} is the perturbed elastic angular rotation of panel i about the y axis and the displacement rate has been taken to be zero: $\dot{d}_i = 0$.

Fig. 5 Correlation of theory and tunnel data for the angle of attack stability derivatives of the Boeing 707-320B (rigid).

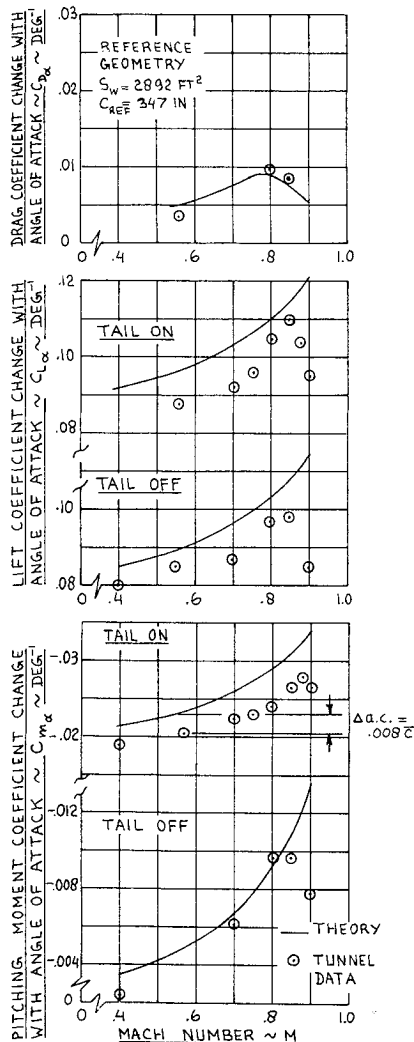
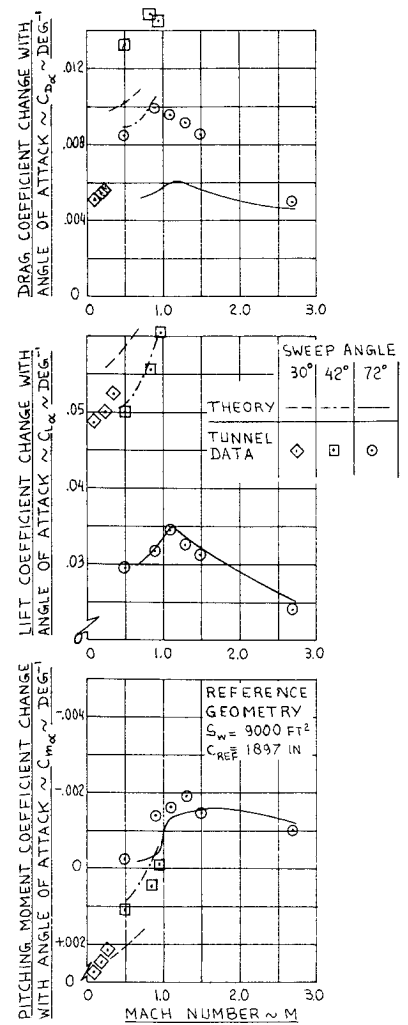


Fig. 6 Correlation of theory and tunnel data for the angle of attack stability derivatives of an SST configuration (rigid).



Elastic deformation of the airplane is caused by aerodynamic, gravitational and inertial forces. In the following, it is assumed that loads and deformations are in phase with each other. The symbols $\{f_{\theta i}\}$ and $\{f_{Ii}\}$ are introduced for gravitational and inertial perturbation forces along the z axis. Now, using the structural influence coefficient theory of Sec. 3, it is possible to relate the perturbed elastic deformation $\{\theta_{Ei}\}$ to the applied perturbed forces as follows:

$$\{\theta_{Ei}\} = [C_{\theta}]\{f_{Ai} - f_{\theta i} - f_{Ii}\} \quad (25)$$

This assumes that the perturbed forces, f_{Ai} , $f_{\theta i}$, and f_{Ii} are all perpendicular to XO (Fig. 2), which is reasonable because the entire theory presented here is valid only for small angles.

It may be shown that the gravitational perturbation forces along Z can be written as:

$$\{f_{\theta i}\} = \{m_i\}g\theta \sin\theta_i \quad (26)$$

For the perturbed inertial forces, it may be shown that, starting from steady-state rectilinear flight,

$$\{f_{Ii}\} = [m_i][\{1\}(\dot{w} - qU_1) - \{x_i\}\dot{q}] \quad (27)$$

Upon introducing Eqs. (24) and (25) into Eq. (23),

$$\{f_{Ai}\} = \bar{q}_1[(2/U_1)[A] + (M_1/U_1)[\partial A/\partial M]]\{\alpha_{Ei}\}u + \bar{q}_1[A][\alpha\{1\} - q/U_1\{x_i\} + [C_{\theta}]\{f_{Ai} - f_{\theta i} - f_{Ii}\}] \quad (28)$$

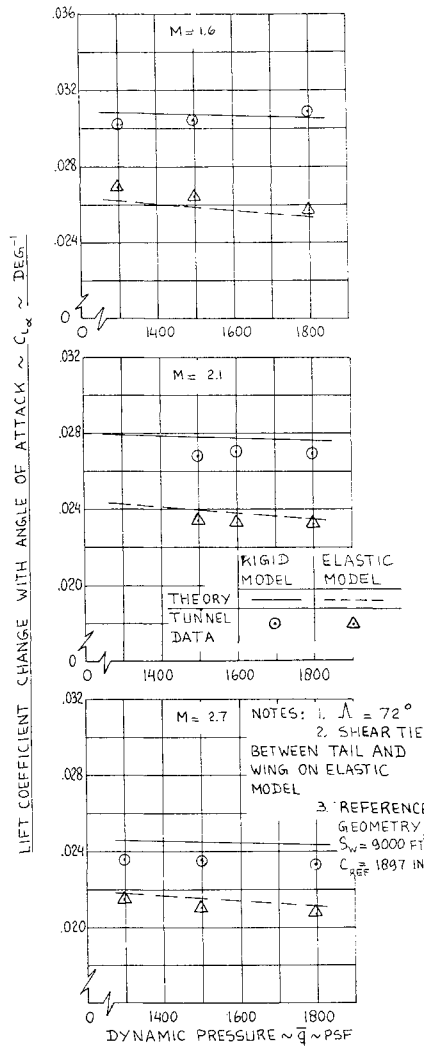


Fig. 7 Correlation of theory and tunnel data for lift curve slope of an elastic SST model.

Solving for $\{f_{Ai}\}$ and introducing the new matrix

$$[B] = [\tilde{1}] - q_1[A][C\theta]^{-1} \quad (29)$$

It is found after substitution of Eq. (26) and Eq. (27) into Eq. (28) that

$$\begin{aligned} \{f_{Ai}\} = & \tilde{q}_1[B][(2/U_1)[A] + M_1/U_1][\partial A/\partial M] \times \\ & \{\alpha_{Ei}\}u + \tilde{q}_1[B][A][\alpha\{1\} - (q/U_1)\{x_i\} - \\ & [C\theta]\{m_i\}g\theta \sin\theta_1 - [C\theta][m_i]\{1\}(\dot{w} - qU_1) - \\ & \{x_i\}q] \quad (30) \end{aligned}$$

Observe that the perturbed panel forces of the elastic airplane depend on the following perturbation variables: u , α , $q = \dot{\theta}$, θ , $\dot{q} = \ddot{\theta}$, and \dot{w} . For a rigid airplane $[C\theta] = 0$ and $[B] = [\tilde{1}]$. Therefore, for a rigid airplane, the perturbed panel forces depend only on the perturbation variables, u , α , and q . Perturbation forces due to θ , \dot{w} , and $\ddot{\theta}$ are all identified with the mass distribution $\{m_i\}$ of the airplane. For that reason, they are called inertial forces.

From Eq. (30), it is now possible to write expressions for the total perturbed force and moment coefficients for the elastic airplane. For small angles, the result is

$$C_{x_s} = f_{Ax_s}/\tilde{q}_1 S_w, C_{z_s} = f_{Az_s}/\tilde{q}_1 S_w, C_m = M_{Ax_m}/\tilde{q}_1 S_w \bar{c} \quad (31)$$

By differentiation of the coefficients, C_{x_s} , C_{z_s} , and C_m with

respect to the perturbation variables, u , α , q , θ , $\dot{\theta}$, and \dot{w} , it is now possible to write the stability derivatives of the airplane, as in Table 1.

Observe from Table 1 that there is an inertial part to all q derivatives for the elastic airplane. It is evident that the rigid airplane has no mass dependent stability derivatives.

The inertial derivatives or derivative components due to θ , q , $\dot{\theta}$, and \dot{w} can be very significant. This is demonstrated for the inertial derivative $C_{m\dot{\theta}}$ in Table 2, where the effect of $C_{m\dot{\theta}}$ is compared with the rigid airplane pitch inertia I_{yy} .

To validate the method presented here, several stability derivatives were calculated for a rigid and an elastic model of a typical SST configuration and compared with corresponding tunnel data. The same was done for a rigid Boeing 707-320B model. Results are presented and discussed in Sec. 5.

5. Comparison with Wind-Tunnel Data

To validate the theory presented in Sec. 4, a comparison has been made between rigid and elastic airplane derivatives as computed from the equations in Table 1 and as determined from wind-tunnel data. Because no tunnel data were available for pitch rate derivatives, the comparison was made only for α and u derivatives.

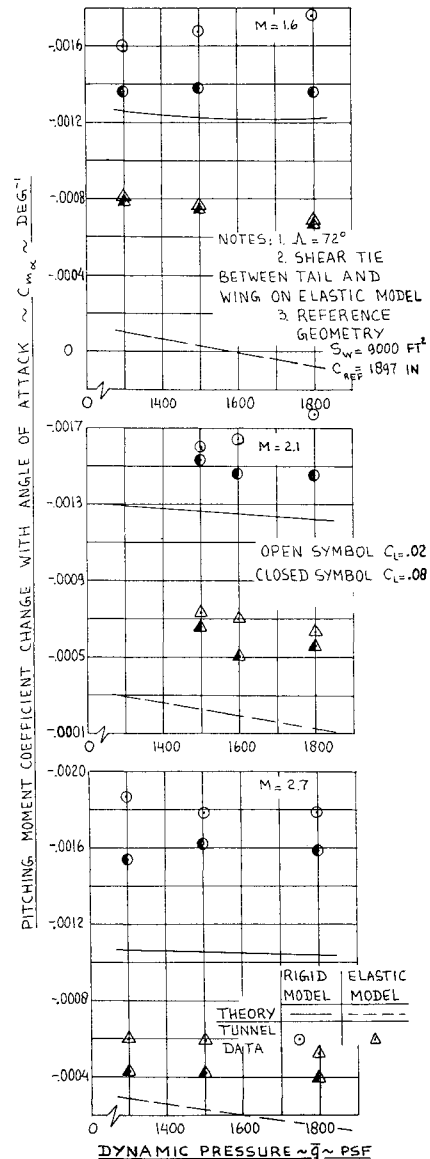


Fig. 8 Correlation of theory and tunnel data for static stability of an elastic SST model.

Table 2 Comparison of $C_{m\dot{\theta}}$ with pitch inertia

707-320B <i>M</i>		Alt., ft	I_{yy} , 10 ⁶ slug·ft ² (Approx.)		$C_{m\dot{\theta}}$ $I_{yy}/\bar{q}S_w\bar{c}$
0.365		10,000	5.025		0.052
0.548		10,000	5.025		0.105
0.800		35,000	5.025		0.094
0.850		35,000	5.025		0.106

SST <i>M</i>	Alt., ft	Gross weight, lb	Wing sweep, deg	I_{yy} , 10 ⁶ slug·ft ² (Approx.)	$C_{m\dot{\theta}}$ $I_{yy}/\bar{q}S_w\bar{c}$
0.5	9,600	370,000	34	40.2	0.0248
0.7	11,000	370,000	30	40.2	0.0217
0.7	26,000	675,000	42	47.2	0.0125
0.9	23,500	675,000	42	47.2	0.0198
1.5	24,000	520,000	72	47.6	0.182
2.2	60,500	520,000	72	47.6	0.0939
2.7	49,000	520,000	72	47.6	0.263

The airplanes used in this comparison are the Boeing 707-320B and a typical SST configuration. Geometric data for both are summarized in Fig. 1.

Figures 3, 4, 5, and 6 show that there is in general quite good correlation between the theoretical and experimental values of the u and α derivatives for rigid configurations. The $C_{D\alpha}$ and C_{Du} correlations were not expected to be good because the aerodynamic representation used in setting up the aerodynamic influence coefficient matrix does not account for the precise leading edge camber while the effects of thickness were also neglected.

For the elastic SST model of Ref. 4, it is shown in Fig. 7 that the correlation between theory and experiment for calculating $C_{L\alpha}$ is good. Figure 8 shows that the agreement between theory and experiment depends on angle of attack (lift coefficient). For the higher lift coefficient values the agreement is fair. No drag or u -derivative data were obtained for this case.

The variation of $C_{L\alpha}$ and $C_{m\alpha}$ with dynamic pressure for the rigid model in Figs. 7 and 8 is caused by the fact that the so-called rigid model in reality is not very rigid. The elastic

properties of this so-called rigid model were accounted for in the corresponding predictions.

On the basis of these correlations, it appears that the theory presented here is capable of predicting α and u derivatives with good accuracy. It is expected that theoretical values for q derivatives will also correlate well with experimental values, once these become available.

6. Conclusions

A method has been presented for predicting longitudinal stability derivatives of arbitrary rigid and elastic airplane configurations. Correlation with wind-tunnel data is generally good. The method applies within the approximate Mach range of $0 < M < 0.80$ and $1.2 < M < 5$. Although no substantiating data are available the authors believe it reasonable to expect that this method will give accurate results for calculating the q -stability derivatives.

The method is particularly useful in predicting the effect of configuration changes during preliminary design. In addition, with this method, it is possible to generate parametric data for the graphical estimation of all stability derivatives for which the method applies.

Finally, the method allows a realistic appraisal of inertial derivatives.

References

- ¹ Gainer, P. A. and Aiken, W. S., Jr., "Modified Matrix Method for Calculating Steady-State Span Loading on Flexible Wings in Subsonic Flight," Memo 5-26-59L, June 1959, NACA.
- ² Woodward, F. A., "A Unified Approach to the Analysis and Design of Wing-Body Combinations at Subsonic and Supersonic Speeds," *Journal of Aircraft*, Vol. 5, No. 6, Nov.-Dec. 1968, pp. 528-534.
- ³ Members of the Aerodynamics and Structures Research Organization of The Boeing Company, "An Analysis of Methods for Predicting the Stability Characteristics of an Elastic Airplane," CR-73277, Nov. 1968, NACA.
- ⁴ Roskam, J., Holgate, T., and Shimizu, G., "Elastic Wind-Tunnel Models for Predicting Longitudinal Stability Derivatives of Elastic Airplanes," *Journal of Aircraft*, Vol. 5, No. 6, Nov.-Dec. 1968, pp. 543-550.